

Two-Loop Electroweak Corrections to the $A^0\gamma\gamma$ and A^0gg Couplings of the CP-Odd Higgs Boson

JOACHIM BROD

Institut für Theoretische Teilchenphysik, Universität Karlsruhe
Engesserstraße 7, 76128 Karlsruhe, Germany

FRANK FUGEL

Paul Scherrer Institut,
5232 Villigen PSI, Switzerland

BERND A. KNIEHL

II. Institut für Theoretische Physik, Universität Hamburg,
Luruper Chaussee 149, 22761 Hamburg, Germany

Abstract

Using the asymptotic-expansion technique, we compute the dominant two-loop electroweak corrections, of $\mathcal{O}(G_F m_t^2)$, to production and decay via a pair of photons or gluons of the CP-odd Higgs boson A^0 in a two-Higgs-doublet model with low- to intermediate values of the Higgs-boson masses and ratio $\tan\beta = v_2/v_1$ of the vacuum expectation values. We also study the influence of a sequential heavy-fermion generation. The appearance of three γ_5 matrices in closed fermion loops requires special care in the dimensional regularisation of ultraviolet divergences. The finite renormalisation constant for the pseudoscalar current effectively restoring the anticommutativity of the γ_5 matrix, familiar from perturbative quantum chromodynamics, is found not to receive a correction in this order. We also revisit the dominant two-loop electroweak correction to the $H \rightarrow \gamma\gamma$ decay width in the standard model with a fourth fermion generation.

PACS numbers:12.15.Lk, 13.66.Fg, 13.85.-t, 14.80.Cp



1 Introduction

The search for Higgs bosons is among the prime tasks at the Fermilab Tevatron and will be so at the CERN Large Hadron Collider (LHC), to go into operation later during this year, and the International e^+e^- Linear Collider (ILC), which is currently being designed. The standard model (SM) contains one complex Higgs doublet, from which one neutral CP-even Higgs boson (H) emerges in the physical particle spectrum after the electroweak symmetry breaking. Despite its enormous success in describing almost all experimental particle physics data available today, the SM is widely believed to be an effective field theory, valid only at presently accessible energy scales, mainly because of the naturalness problem related to the fine-tuning of the cut-off scale appearing quadratically in the Higgs-boson mass counterterm, the failure of gauge coupling unification, the absence of a concept to incorporate gravity, and the lack of a cold-dark-matter candidate. Supersymmetry (SUSY), which postulates the existence of a partner, with spin shifted by half a unit, to each of the established matter and exchange particles, is commonly viewed as the most attractive extension of the SM solving all these problems. The Higgs sector of the minimal SUSY extension of the SM (MSSM) consists of a two-Higgs-doublet model (2HDM) and accommodates five physical Higgs bosons: the neutral CP-even h^0 and H^0 bosons, the neutral CP-odd A^0 boson, and the charged H^\pm -boson pair. At the tree level, the MSSM Higgs sector has two free parameters, which are usually taken to be the mass M_{A^0} of the A^0 boson and the ratio $\tan\beta = v_2/v_1$ of the vacuum expectation values of the two Higgs doublets.

The discovery of the A^0 boson would rule out the SM and, at the same time, give strong support to the MSSM. At the LHC, this will be feasible except in the wedge of parameter space with $M_{A^0} \gtrsim 250$ GeV and moderate value of $\tan\beta$, where only the h^0 boson can be detected [1]. For low to intermediate values of $\tan\beta$, gluon fusion is by far the dominant hadroproduction mechanism. At large values of $\tan\beta$, $A^0 b\bar{b}$ associated production becomes important, too, especially at LHC c.m. energy, $\sqrt{s} = 14$ TeV [2,3]. At the ILC operated in the $\gamma\gamma$ mode, via Compton back-scattering of highly energetic laser light off the electron and positron beams, single production of the A^0 boson will allow for its discovery, also throughout a large fraction of the LHC wedge, and for a precision determination of its profile [4]. Two-photon collisions, albeit with less luminosity, will also take place in the regular e^+e^- mode of the ILC through electromagnetic bremsstrahlung or beamstrahlung off the lepton beams.

In the mass range $M_{A^0} < 2m_t$ and for large values of $\tan\beta$ in the whole M_{A^0} range, the A^0 boson dominantly decays to a $b\bar{b}$ pair, with a branching fraction of about 90% [2,3]. As in the case of the H boson of the SM, the rare $\gamma\gamma$ decay channel then provides a useful signature at the LHC if the b and \bar{b} quarks cannot be separated sufficiently well from the overwhelming background from quantum chromodynamics (QCD). The $A^0 \rightarrow gg$ channel will greatly contribute to the decay mode to a light-hadron dijet, which will be measurable at the ILC.

Since the A^0 boson is neutral and colourless, the $A^0\gamma\gamma$ and A^0gg couplings are loop induced. As the A^0 boson has no tree-level coupling to the W boson and its coupling to

sfermions flips their “handedness” (left or right), the $A^0\gamma\gamma$ coupling is mediated at leading order (LO) by heavy quarks and charged leptons and by light charginos, whereas heavy charginos decouple [5]. The A^0gg coupling is generated at LO by heavy-quark loops [6].

Reliable theoretical predictions for the $A^0\gamma\gamma$ and A^0gg couplings, including higher-order radiative corrections, are urgently required to match the high precision to be reached by the LHC and ILC experiments [7,8]. Specifically, the properties of the A^0 boson, especially its CP-odd nature, must be established, and the sensitivity to novel high-mass particles circulating in the loops must be optimised. The present state of the art is as follows. The next-to-leading-order (NLO) QCD corrections, of relative order $\mathcal{O}(\alpha_s)$ in the strong-coupling constant α_s , to the partial decay widths $\Gamma(A^0 \rightarrow \gamma\gamma)$ [9,10] and $\Gamma(A^0 \rightarrow gg)$ [10], and the production cross section $\sigma(gg \rightarrow A^0)$ [10,11] are available for arbitrary values of quark and A^0 -boson masses as one-dimensional integrals, which were solved in terms of harmonic polylogarithms for $\Gamma(A^0 \rightarrow \gamma\gamma)$, $\Gamma(A^0 \rightarrow gg)$, and the virtual correction to $\sigma(gg \rightarrow A^0)$ [12,13]. The latter was also obtained for general colour factors of the gauge group $SU(N_c)$ in the limit $m_t \rightarrow \infty$ using an effective Lagrangian [14]. In the same way, the $\mathcal{O}(\alpha_s)$ correction to $\sigma(gg \rightarrow A^0)$ was first calculated in Ref. [15].

The next-to-next-to-leading-order (NNLO) QCD corrections, of $\mathcal{O}(\alpha_s^2)$, to $\Gamma(A^0 \rightarrow gg)$ [16] and $\sigma(gg \rightarrow A^0)$ [17] were found for $m_t \rightarrow \infty$ using an effective Lagrangian. The $\mathcal{O}(\alpha_s)$ SUSY QCD correction, due to virtual squarks and gluinos besides the heavy quarks, to $\sigma(gg \rightarrow A^0)$ was obtained from an effective Lagrangian constructed by also integrating out the SUSY particles [18]. The two-loop master integrals appearing in the latter calculation if the masses of the virtual scalar bosons and fermions are kept finite were expressed in terms of harmonic polylogarithms [13].

In this paper, we take the next step and present the dominant electroweak corrections to $\Gamma(A^0 \rightarrow \gamma\gamma)$ and $\Gamma(A^0 \rightarrow gg)$ at NLO. Our key results were already summarised in Ref. [19]. Here, we present the full details of our calculation and a comprehensive discussion of its phenomenological implications. Since these corrections are purely virtual, arising from two-loop diagrams, they carry over to $\sigma(\gamma\gamma \rightarrow A^0)$ and $\sigma(gg \rightarrow A^0)$, via

$$\sigma(\gamma\gamma/gg \rightarrow A^0) = \frac{8\pi^2}{N_{\gamma,g}^2 M_{A^0}} \Gamma(A^0 \rightarrow \gamma\gamma/gg) \delta(\hat{s} - M_{A^0}^2), \quad (1)$$

where $N_\gamma = 1$ and $N_g = N_c^2 - 1 = 8$ are the colour multiplicities of the photon and the gluon, respectively, and \hat{s} is the partonic c.m. energy square. For the time being, we focus our attention on the particularly interesting region of parameter space with low to intermediate Higgs-boson masses, $M_{h^0}, M_{H^0}, M_{A^0}, M_{H^\pm} < m_t$,¹ and low to moderate value of $\tan\beta$, $\tan\beta \ll m_t/m_b$, and assume that the SUSY particles are so heavy that they can be regarded as decoupled, yielding subdominant contributions. The dominant electroweak two-loop corrections are then induced by the top quark and are of relative order $\mathcal{O}(x_t)$, where $x_t = G_F m_t^2 / (8\pi^2 \sqrt{2}) \approx 3.17 \times 10^{-3}$ with G_F being Fermi’s constant. We also consider the influence of a sequential generation of heavy fermions F , beyond the

¹As for M_{A^0} , we actually need $M_{A^0} < 2M_{W^\pm}, 2M_{H^\pm}$ in order for asymptotic expansion to be applicable.

established three generations, which generate corrections of generic order $\mathcal{O}(x_F)$. Such corrections were already studied for the $H \rightarrow \gamma\gamma$ decay in the SM supplemented with a fourth fermion generation in Ref. [20], and we revisit this analysis.

In the calculation of two-loop electroweak corrections to the $A^0\gamma\gamma$ and A^0gg couplings, one encounters closed fermion loops involving three γ_5 matrices, so that the use of the naïve anticommuting definition of the γ_5 matrix is bound to fail. This leads us to employ the 't Hooft-Veltman-Breitenlohner-Maison (HVBM) [21] scheme and a finite renormalisation constant, Z_5^p , for the pseudoscalar current to effectively restore the anticommutativity of the γ_5 matrix [22,23,24], which is so far only known within QCD [24].

This paper is organised as follows. In Section 2, we explain our method of calculation and evaluate Z_5^p to $\mathcal{O}(x_t)$ and $\mathcal{O}(x_F)$. In Section 3, we calculate the $\mathcal{O}(x_t)$ and $\mathcal{O}(x_F)$ corrections to $\Gamma(A^0 \rightarrow \gamma\gamma)$ and $\Gamma(A^0 \rightarrow gg)$ in the 2HDM with three and four fermion generations. We also recover the $\mathcal{O}(\alpha_s)$ correction to $\Gamma(A^0 \rightarrow \gamma\gamma)$. In Section 4, we recalculate the $\mathcal{O}(x_F)$ correction to $\Gamma(H \rightarrow \gamma\gamma)$ due to a fourth fermion generation added on top of the SM. In Section 5, we present our numerical results. We conclude with a summary in Section 6.

2 Method of calculation

As explained below, we assume a strong hierarchy between the heavy fermions on the one hand and the gauge and Higgs bosons on the other hand, so that we may extract the leading corrections using the asymptotic-expansion technique [25]. We use a completely automated set-up, which relies on the successive use of the computer programs QGRAF [26], q2e, exp [27], and MATAD [28]. First, QGRAF is used to generate the Feynman diagrams. Its output is then rewritten by q2e to be understandable by exp. The latter performs the asymptotic expansion and generates the relevant subdiagrams according to the rules of the so-called hard-mass procedure [25]. Form [29] files are generated. They can be read by MATAD, which performs the calculation of the diagrams.

Since we consider the SUSY partners to be decoupled, we may as well work in the 2HDM without SUSY. We may thus extract the ultraviolet (UV) divergences by means of dimensional regularisation, with $d = 4 - 2\epsilon$ space-time dimensions and 't Hooft mass scale μ , without introducing SUSY-restoring counterterms [30]. For convenience, we work in 't Hooft-Feynman gauge. We take the Cabibbo-Kobayashi-Maskawa quark mixing matrix to be unity, which is well justified because the third quark generation is, to good approximation, decoupled from the first two [31]. We adopt Sirlin's formulation of the electroweak on-shell renormalisation scheme [32], which uses G_F and the physical particle masses as basic parameters, and its extension to the MSSM [33]. Various prescriptions for the renormalisation of the auxiliary variable $\tan\beta$, with specific virtues and flaws, may be found in the literature, none of which is satisfactory in all respects (for a review, see Ref. [34]). For definiteness, we employ the Dabelstein-Chankowski-Pokorski-Rosiek (DCPR) scheme [35,36], which maintains the relation $\tan\beta = v_2/v_1$ in terms of the "true" vacua through the condition $\delta v_1/v_1 = \delta v_2/v_2$, and demands the residue condition

$\text{Re } \hat{\Sigma}'_{A^0}(M_{A^0}) = 0$ and the vanishing of the A^0 - Z^0 mixing on shell as $\text{Re } \hat{\Sigma}_{A^0 Z^0}(M_{A^0}) = 0$, where $\hat{\Sigma}_{A^0}(q^2)$ and $\hat{\Sigma}_{A^0 Z^0}(q^2)$ are the renormalised A^0 -boson self-energy and A^0 - Z^0 mixing amplitude, respectively. It has been pointed out [34] that the DCPR definition of $\tan \beta$ is gauge dependent. We do not actually encounter this drawback in our analysis, since we need to renormalise $\tan \beta$ to $\mathcal{O}(x_f)$, so that only fermion loops contribute. However, this problem will show up when subleading terms of the two-loop electroweak corrections are to be computed. Our final results can be straightforwardly converted to any other renormalisation prescription for $\tan \beta$, by substituting the finite relationship between the old and new definitions of $\tan \beta$.

As already mentioned in Section 1, the evaluation of the relevant two-loop diagrams is aggravated by the appearance of three γ_5 matrices inside closed fermion loops. This leads us to adopt the HVBM scheme [21], which allows for a consistent treatment of the Dirac algebra within the framework of dimensional regularisation. In this scheme, the γ_5 matrix is given by

$$\gamma_5 = \frac{i}{4!} \varepsilon_{\mu\nu\rho\sigma} \gamma^\mu \gamma^\nu \gamma^\rho \gamma^\sigma, \quad (2)$$

where the totally antisymmetric Levi-Civita tensor is defined in d dimensions as

$$\varepsilon_{\mu\nu\rho\sigma} = \begin{cases} 1 & \text{if } (\mu, \nu, \rho, \sigma) \text{ even permutations of } (0,1,2,3), \\ -1 & \text{if } (\mu, \nu, \rho, \sigma) \text{ odd permutations of } (0,1,2,3), \\ 0 & \text{otherwise.} \end{cases} \quad (3)$$

This definition leads to the following mixed anticommutation and commutation relations, where we have to distinguish between 4 and $(d-4)$ dimensions:

$$\begin{aligned} \{\gamma^\mu, \gamma_5\} &= 0, & \text{if } \mu = 0, 1, 2, 3, \\ [\gamma^\mu, \gamma_5] &= 0, & \text{otherwise.} \end{aligned} \quad (4)$$

By giving up the full anticommutation property of γ_5 , we can retain the familiar expression for the trace of four γ matrices and one γ_5 matrix:

$$\text{tr}(\gamma_\mu \gamma_\nu \gamma_\rho \gamma_\sigma \gamma_5) = 4i \varepsilon_{\mu\nu\rho\sigma}. \quad (5)$$

Traces involving less than four γ matrices and one γ_5 matrix vanish. We introduce the following projectors onto the 4- and $(d-4)$ -dimensional subspaces:

$$\begin{aligned} \tilde{g}^{\mu\nu} &= \begin{cases} g^{\mu\nu} & \text{if } \mu \text{ and } \nu \text{ are smaller than } 4, \\ 0 & \text{otherwise;} \end{cases} \\ \hat{g}^{\mu\nu} &= \begin{cases} g^{\mu\nu} & \text{if } \mu \text{ and } \nu \text{ are larger than } 3, \\ 0 & \text{otherwise.} \end{cases} \end{aligned} \quad (6)$$

Here and in the following, we label quantities in 4 dimensions with a tilde, quantities in $(d-4)$ dimensions with a hat, and quantities in d dimensions without superscript. For a

given four-vector V , we thus have

$$\begin{aligned}\tilde{V}^\mu &= \tilde{g}^{\mu\nu} V_\nu, \\ \hat{V}^\mu &= \hat{g}^{\mu\nu} V_\nu.\end{aligned}\tag{7}$$

The projectors fulfil the following relations:

$$\begin{aligned}\tilde{g}_\mu^\mu &= g^{\mu\nu} \tilde{g}_{\mu\nu} = \tilde{g}^{\mu\nu} \tilde{g}_{\mu\nu} = 4, \\ \hat{g}_\mu^\mu &= g^{\mu\nu} \hat{g}_{\mu\nu} = \hat{g}^{\mu\nu} \hat{g}_{\mu\nu} = d - 4, \\ \tilde{g}^{\mu\nu} \hat{g}_{\mu\nu} &= 0.\end{aligned}\tag{8}$$

More details may be found in Ref. [23]. We explicitly verified that, in our case, the naïve anticommuting definition of the γ_5 matrix yields ambiguous results, which depend on the way of executing the Dirac traces.

The actual implementation of these rules into the **MATAD** setup is accomplished in two independent ways. Firstly, we use the **Mathematica** package **TRACER** [37] and compute the traces separately. Secondly, we implement our own **FORM** routine for evaluating the traces in the HVBM scheme. Both methods yield the same results.

The application of the HVBM scheme introduces loop momenta that are projected onto the $(d - 4)$ -dimensional subspace. These have to be expressed through loop momenta in the full d -dimensional space because **MATAD** performs the integration in d dimensions. For instance, in the case of a massive one-loop tadpole with loop momentum q , we substitute

$$\hat{q}^2 = \frac{4}{d} q^2\tag{9}$$

in the numerator of the integrand. Similar identities can be derived for all the other cases.

Furthermore, we have to introduce an additional finite counterterm, Z_5^p , in the renormalisation of the pseudoscalar current to effectively restore the anticommutativity of the γ_5 matrix [22,23,24]. Within QCD, Z_5^p is known through $\mathcal{O}(\alpha_s^3)$ [24]. Here, we need Z_5^p at $\mathcal{O}(x_t)$ and $\mathcal{O}(x_F)$. In order to explain our procedure, we first repeat the derivation of the $\mathcal{O}(\alpha_s)$ term. For simplicity, we work in massless QCD with 't Hooft-Feynman gauge. As usual, we adopt the modified minimal-subtraction ($\overline{\text{MS}}$) renormalisation scheme. The pseudoscalar current is defined in coordinate space as

$$P(x) = Z_2 Z^p Z_5^p \bar{\psi}(x) \gamma_5 \psi(x),\tag{10}$$

where Z_2 and Z^p are the usual wave-function and pseudoscalar-current renormalisation constants, respectively. Passing to momentum space, we define

$$iS_F(p) \Gamma_5(p, p') iS_F(p') = \int d^d x d^d y e^{i(p \cdot x - p' \cdot y)} \langle 0 | T[\psi(x) P(0) \bar{\psi}(y)] | 0 \rangle,\tag{11}$$

where T denotes the time-ordered product and $iS_F(p) = \int d^d x e^{ip \cdot x} \langle 0 | T[\psi(x) \bar{\psi}(0)] | 0 \rangle$ is the Feynman propagator of the quark. The key quantity for our purposes is then the

amputated Green function $\Gamma_5(p, p)$ at zero momentum transfer. The Feynman diagrams relevant through $\mathcal{O}(\alpha_s)$ are depicted in Fig. 1, where crosses and dots indicate the insertions of $P(x)$ and the operator renormalisation, respectively, and it is understood that external legs are amputated. The tree-level diagram in Fig. 1(a) yields

$$\Gamma_5^{(0)}(p, p) = \gamma_5. \quad (12)$$

The one-loop diagram in Fig. 1(b) leads to the integral

$$\Gamma_5^{(1)}(p, p) = 4\pi\alpha_s C_F \int \frac{d^d q}{(2\pi)^d} \frac{-i\gamma_\mu \not{q} \gamma_5 \not{q} \gamma^\mu}{(p-q)^2 (q^2)^2}, \quad (13)$$

where $C_F = (N_c^2 - 1)/(2N_c) = 4/3$ is the eigenvalue of the Casimir operator of the fundamental representation of $SU(N_c)$, with $N_c = 3$ for QCD. We decompose the string of gamma matrices in the numerator as

$$\gamma_\mu \not{q} \gamma_5 \not{q} \gamma^\mu = \gamma_\mu \not{q} \not{q} \gamma^\mu \gamma_5 + \gamma_\mu \not{q} (-2\not{q} \hat{\gamma}^\mu - 2\not{q} \gamma^\mu + 4\not{q} \hat{\gamma}^\mu) \gamma_5. \quad (14)$$

The first term on the right-hand side of Eq. (14) is what we would obtain using an anticommuting γ_5 matrix. Upon loop integration it yields an expression proportional to Eq. (12), the divergent part of which is

$$\Gamma_5^{(1), \text{div}}(p, p) = \frac{\alpha_s}{\pi} C_F \frac{1}{\epsilon} \gamma_5. \quad (15)$$

This is removed by Fig. 1(c), the $\mathcal{O}(\alpha_s)$ terms of Z_2 and Z^p being [24]

$$\begin{aligned} Z_2 &= 1 - \frac{\alpha_s}{\pi} C_F \frac{1}{4\epsilon}, \\ Z^p &= 1 - \frac{\alpha_s}{\pi} C_F \frac{3}{4\epsilon}. \end{aligned} \quad (16)$$

The remaining terms on the right-hand side of Eq. (14) are evanescent; they live in the unphysical $(d-4)$ -dimensional part of space-time and vanish if we let $d \rightarrow 4$. Yet the loop integral is divergent, so that an unphysical finite contribution remains. We can ensure the vanishing of such contributions to all orders by a finite renormalisation. This is exactly what is achieved by the finite renormalisation Z_5^p . In this way, we ensure that the evanescent part does not mix into the physical part. Upon loop integration, the evanescent part of Eq. (14) yields

$$\Gamma_5^{(1), \text{eva}}(p, p) = 2 \frac{\alpha_s}{\pi} C_F \gamma_5, \quad (17)$$

so that, through $\mathcal{O}(\alpha_s)$, the finite counterterm is

$$Z_5^p = 1 + \delta Z_5^p = 1 - 2 \frac{\alpha_s}{\pi} C_F, \quad (18)$$

in agreement with Ref. [24].

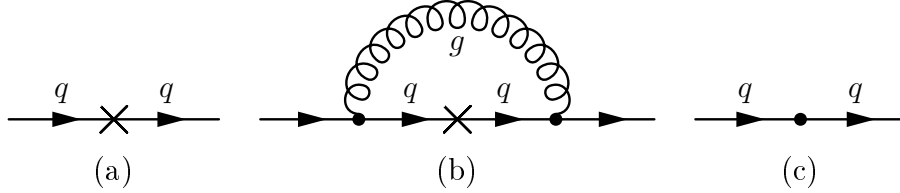


Figure 1: Feynman diagrams contributing to Z_5^p at $\mathcal{O}(\alpha_s)$. Crosses and dots indicate insertions of $P(x)$ and its operator renormalisation $Z_2 Z^p Z_5^p$, respectively.

We now apply the same procedure at $\mathcal{O}(x_t)$ and $\mathcal{O}(x_F)$. To this end, we have to consider the counterparts of the diagram in Fig. 1(b) where the gluon is replaced by neutral or charged scalar electroweak bosons, $S^0 = \chi^0, h^0, H^0, A^0$ and $S^\pm = \phi^\pm, H^\pm$, where χ^0 and ϕ^\pm denote the Goldstone bosons. These are depicted in Figs. 2(a) and (b), respectively. We find that the sets of diagrams in Figs. 2(a) and (b) add up to zero separately. In the three-generation case, the diagrams in Figs. 2(b) do not contribute in $\mathcal{O}(x_t)$ at all. Consequently, we have $\delta Z_5^p = 0$ at $\mathcal{O}(x_t)$ and $\mathcal{O}(x_F)$.

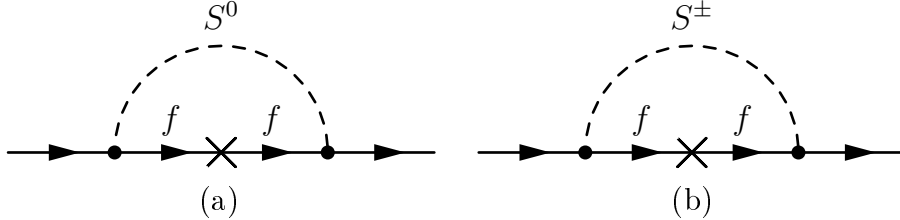


Figure 2: Feynman diagrams contributing to Z_5^p at $\mathcal{O}(x_t)$ and $\mathcal{O}(x_F)$. Crosses indicate insertions of $P(x)$, and $S^0 = \chi^0, h^0, H^0, A^0$, $S^\pm = \phi^\pm, H^\pm$, and $f = t, b, U, D, N, E$ denote generic neutral and charged scalar bosons and fermions, respectively.

3 $A^0 \rightarrow \gamma\gamma$ and $A^0 \rightarrow gg$

In this section, we first discuss the case of $A^0 \rightarrow \gamma\gamma$ in detail. Specifically, we recall the Born result and recover the $\mathcal{O}(\alpha_s)$ correction in Subsection 3.1 and evaluate the $\mathcal{O}(x_t)$ and $\mathcal{O}(x_F)$ corrections in Subsection 3.2. In Subsection 3.3, we then extract from the latter the corresponding corrections for $A^0 \rightarrow gg$.

We drop all terms including an even number of γ_5 matrices in the fermion trace, since they do not give contributions to the final results. Those with an odd number lead to expressions that are proportional to the epsilon tensor. The transition amplitude can thus be decomposed as follows:

$$\mathcal{T} = \frac{1}{4!} \varepsilon_{\alpha\beta\gamma\delta} \epsilon_\mu^*(q_1) \epsilon_\nu^*(q_2) \mathcal{A}^{\mu\nu\alpha\beta\gamma\delta}, \quad (19)$$

where q_i and $\epsilon^*(q_i)$ are the four-momenta and polarisation four-vectors of the outgoing photons $i = 1, 2$. By Lorentz covariance, Eq. (19) can be written as

$$\mathcal{T} = \epsilon^{\mu\nu\rho\sigma} q_{1\mu} q_{2\nu} \epsilon_\rho^*(q_1) \epsilon_\sigma^*(q_2) \mathcal{A}, \quad (20)$$

where

$$\mathcal{A} = -\frac{\tilde{g}_{[\alpha\mu}\tilde{g}_{\beta\nu}g_{\gamma\rho}g_{\delta\sigma]} q_1^\rho q_2^\sigma}{48(q_1 \cdot q_2)^2} \mathcal{A}^{\mu\nu\alpha\beta\gamma\delta}. \quad (21)$$

Here, $[\]_1$ denotes antisymmetrisation in the first indices of the metric tensors, and it is understood that the external momenta q_1 and q_2 have non-vanishing components only in the physical four dimensions of space-time. The partial width of the $A^0 \rightarrow \gamma\gamma$ decay is then given by

$$\Gamma(A^0 \rightarrow \gamma\gamma) = \frac{M_{A^0}^3}{64\pi} |\mathcal{A}|^2. \quad (22)$$

The form factor \mathcal{A} is evaluated in perturbation theory as

$$\mathcal{A} = \sum_f (\mathcal{A}_f^{\text{LO}} + \mathcal{A}_f^{\alpha_s} + \mathcal{A}_f^{x_f} + \dots) + \dots, \quad (23)$$

where the sum is over heavy fermions $f = t, F$, $\mathcal{A}_f^{\text{LO}}$ is the one-loop contribution induced by charged fermions, $\mathcal{A}_f^{\alpha_s}$ is the two-loop QCD correction in the case of f being a quark, $\mathcal{A}_f^{x_f}$ is the dominant two-loop electroweak correction due to weak-isospin doublets of quarks and leptons, and the ellipses stand for the residual one- and two-loop contributions as well as all contributions beyond two loops. The counterpart of Eq. (22) for $\Gamma(A^0 \rightarrow gg)$ contains an additional colour factor of $N_g/4 = 2$ on the right-hand side.

The couplings of the A^0 boson to fermions are proportional to their masses. Therefore, we only consider diagrams where the A^0 boson couples to the top quark or a fourth-generation fermion. However, we must bear in mind that diagrams where it couples to the bottom quark may become sizeable for large values of $\tan\beta$, for $\tan\beta = \mathcal{O}(m_t/m_b)$, because that coupling is proportional to $\tan\beta$. In the following, we thus concentrate on low to intermediate values of $\tan\beta$.

3.1 Born result for $\Gamma(A^0 \rightarrow \gamma\gamma)$ and $\mathcal{O}(\alpha_s)$ correction

The LO result arises from the diagrams shown in Fig. 3 and may be found in Ref. [5] for $d = 4$ space-time dimensions. For $d = 4 - 2\epsilon$ through $\mathcal{O}(\epsilon)$, we have in closed form and as an expansion in $\tau_f = M_{A^0}^2/(2m_f)^2$:

$$\begin{aligned} \mathcal{A}_f^{\text{LO}} &= 2^{1/4} G_F^{1/2} \frac{\alpha_{\text{em}}}{\pi} N_f Q_f^2 g_f \left(\frac{4\pi\mu^2}{m_f^2} e^{-\gamma_E} \right)^\epsilon \left[-\frac{1}{\tau_f} \arcsin^2 \sqrt{\tau_f} + \mathcal{O}(\epsilon) \right] \\ &= 2^{1/4} G_F^{1/2} \frac{\alpha_{\text{em}}}{\pi} N_f Q_f^2 g_f \left(\frac{4\pi\mu^2}{m_f^2} e^{-\gamma_E} \right)^\epsilon \left[-1 - \frac{1}{3}\tau_f - \frac{8}{45}\tau_f^2 - \frac{4}{35}\tau_f^3 - \frac{128}{1575}\tau_f^4 + \mathcal{O}(\tau_f^5) \right. \\ &\quad \left. + \mathcal{O}(\epsilon) \right], \end{aligned} \quad (24)$$

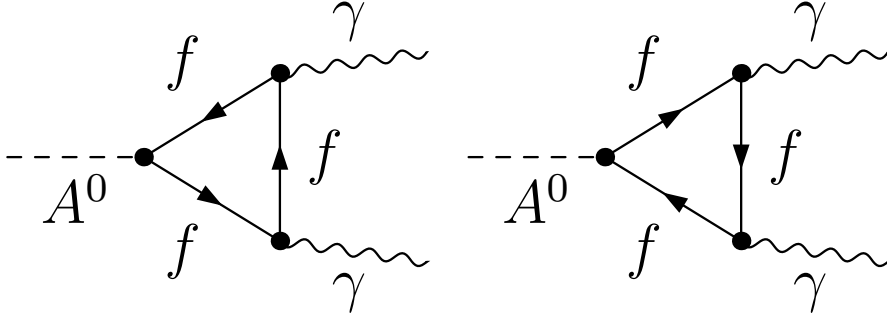


Figure 3: One loop diagrams contributing to $\Gamma(A^0 \rightarrow \gamma\gamma)$. $f = t, b, U, D, N, E$ denotes generic fermions.

where γ_E is the Euler-Mascheroni constant, α_{em} is Sommerfeld's fine-structure constant, $N_f = 1, N_c$ is the colour multiplicity of fermion f , Q_f is its fractional electric charge, and $g_f = \cot \beta, \tan \beta$ for up-type and down-type is its coupling strength to the A^0 boson normalised to its Yukawa coupling in the SM. Note that $M_{A^0}^2$ enters Eq. (24) through the kinematic relation $(q_1 + q_2)^2 = M_{A^0}^2$. The corresponding result for $A^0 \rightarrow gg$ is obtained from Eq. (24) through the substitution $\alpha_{\text{em}} N_f Q_f^2 \rightarrow \alpha_s$.

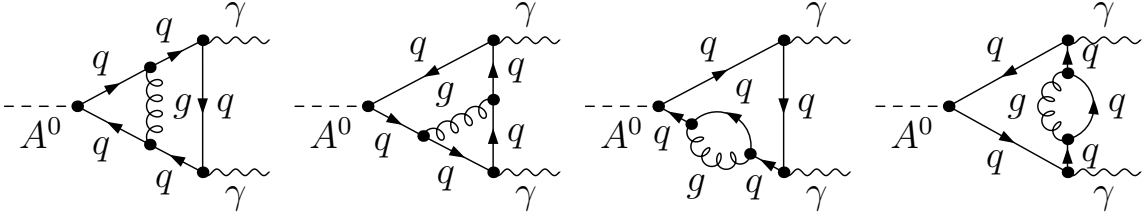


Figure 4: Sample two-loop diagrams contributing to the $\mathcal{O}(\alpha_s)$ QCD corrections to $\Gamma(A^0 \rightarrow \gamma\gamma)$.

We now turn to the $\mathcal{O}(\alpha_s)$ QCD corrections. Besides the proper vertex diagrams, some of which are depicted in Fig. 4, we also need to include the counterterm contribution, so that $\mathcal{A}_q^{\alpha_s} = \mathcal{A}_{q,\text{CT}}^{\alpha_s} + \mathcal{A}_{q,0}^{\alpha_s}$. As for renormalisation, besides including the finite counterterm of the pseudoscalar current in Eq. (18), we only need to renormalise the quark mass appearing in the prefactor of Eq. (24), by shifting its bare value as $m_q^0 = m_q + \delta m_q$, so that

$$\mathcal{A}_{q,\text{CT}}^{\alpha_s} = \mathcal{A}_q^{\text{LO}} \Big|_{\epsilon=0} \left(\delta Z_5^p - 2\epsilon \frac{\delta m_q}{m_q} \right). \quad (25)$$

In the on-shell scheme, the quark mass counterterm is

$$\frac{\delta m_q}{m_q} = \frac{\alpha_s}{\pi} C_F \left(-\frac{3}{4} \Delta - \frac{3}{4} \ln \frac{\mu^2}{m_q^2} - 1 \right), \quad (26)$$

where $\Delta = 1/\epsilon - \gamma_E + \ln(4\pi)$. In total, our evaluation yields

$$\mathcal{A}_q^{\alpha_s} = 2^{1/4} G_F^{1/2} \frac{\alpha_{\text{em}}}{\pi} \frac{\alpha_s}{\pi} N_c Q_q^2 g_q \left[-\frac{16}{9} \tau_q - \frac{68}{45} \tau_q^2 - \frac{53012}{42525} \tau_q^3 - \frac{34712}{33075} \tau_q^4 + \mathcal{O}(\tau_q^5) \right], \quad (27)$$

which agrees with the Taylor expansion of the analytic result derived in Refs. [12,13] from the integral representation originally obtained in Refs. [9,10].

Notice that the $\mathcal{O}(\tau^0)$ term in Eq. (27) vanishes, so that the $\mathcal{O}(\alpha_s)$ correction is suppressed for small values of M_{A^0} . In fact, as a consequence of the Adler-Bardeen theorem [38], the large- m_t effective Lagrangian of the $A^0\gamma\gamma$ interaction does not receive QCD corrections at any order [9,15,39].

3.2 $\mathcal{O}(x_t)$ and $\mathcal{O}(x_F)$ corrections to $\Gamma(A^0 \rightarrow \gamma\gamma)$

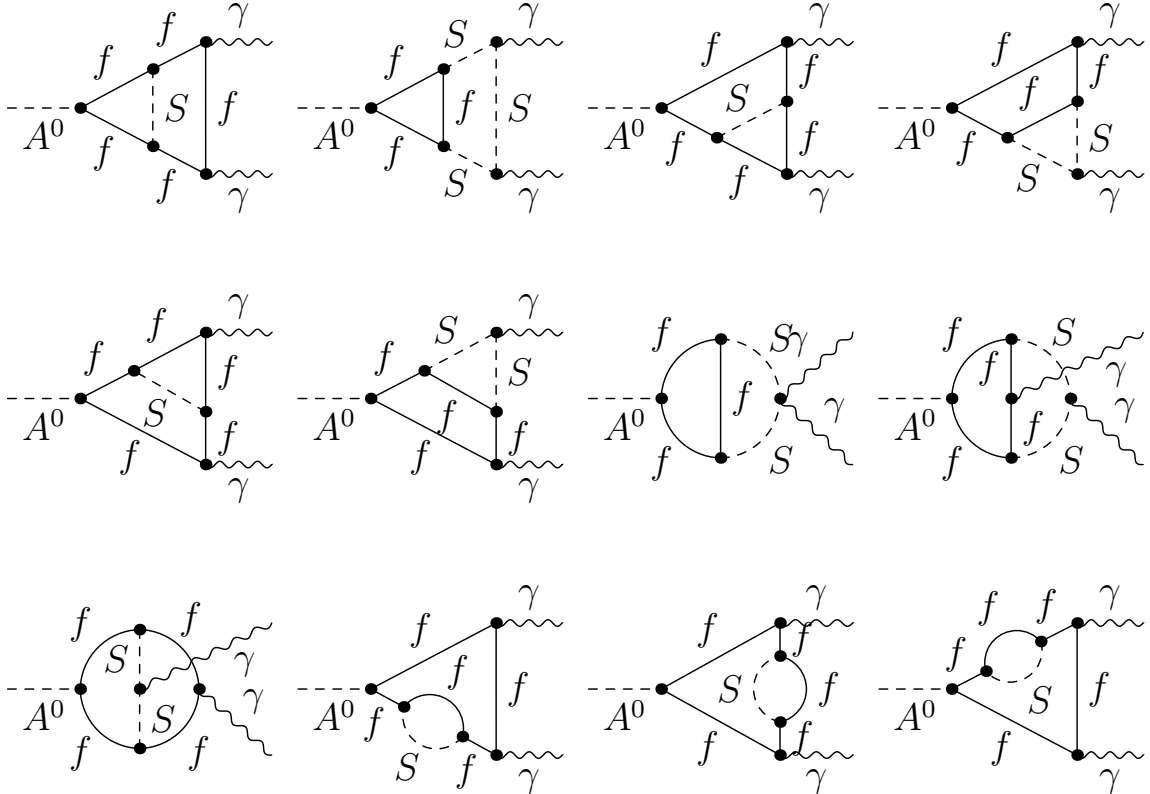


Figure 5: Generic two-loop diagrams contributing to the $\mathcal{O}(x_f)$ electroweak corrections to $\Gamma(A^0 \rightarrow \gamma\gamma)$. $S = \chi^0, \phi^\pm, h^0, H^0, A^0, H^\pm$ and $f = t, b, U, D, N, E$ denote generic scalar bosons and fermions, respectively. The couplings of the neutral scalar bosons to the bottom quark are to be neglected and those of the neutral particles to the photon vanish.

Now we turn to the dominant electroweak two-loop corrections. We first consider the case of three fermion generations. Later on, we also study the additional corrections

induced by a sequential fermion generation, consisting of an up-type quark U , a down-type quark D , a Dirac neutrino N , and a charged lepton E . The contributing diagrams are depicted generically in Fig. 5. We have checked explicitly that diagrams including virtual W bosons do not contribute to our order.

Let us first discuss the counterterm contributions. In contrast to the QCD case in Eq. (25), we now also have to renormalise the A^0 wave function, G_F , and $\tan \beta$. These additional contributions are universal. We thus have

$$\mathcal{A}_{f,\text{CT}}^{x_f} = -2^{1/4} G_F^{1/2} \frac{\alpha_{\text{em}}}{\pi} N_f Q_f^2 g_f \left(\delta Z_5^p - 2\epsilon \frac{\delta m_f}{m_f} + \delta_u \right), \quad (28)$$

where, in the electroweak on-shell scheme [32,33] supplemented with the DCPR [35] definition of $\tan \beta$,

$$\delta_u = \frac{\delta v}{v} - \frac{\Delta r}{2}. \quad (29)$$

Here, $\delta v/v$ is the common DCPR counterterm for the two Higgs doublets given in Eq. (3.11) of Ref. [36] and Δr [32] contains those radiative corrections to the muon lifetime which the SM introduces on top of those derived in the QED-improved Fermi model. In terms of (transverse) self-energies, we have

$$\delta_u = \frac{1}{2} \left[-\frac{\Sigma_{W^\pm, T}(0)}{M_W^2} - \Sigma'_{A^0}(M_{A^0}^2) + (\tan \beta - \cot \beta) \frac{\Sigma_{A^0 Z^0}(M_{A^0}^2)}{M_Z} \right]. \quad (30)$$

In the three-generation case, we set $m_b = 0$ and formally impose the following mass hierarchies:

$$M_Z, M_W, M_{h^0}, M_{H^0}, M_{A^0}, M_{H^\pm} < m_t, \quad M_{A^0} < 2M_W, 2M_{H^\pm}, \quad (31)$$

which ensure the applicability of the asymptotic-expansion technique. In practice, this implies that the unknown Higgs-boson masses obey

$$M_{h^0}, M_{H^0}, M_{A^0}, M_{H^\pm} < m_t, \quad M_{A^0} < 2M_{H^\pm}. \quad (32)$$

The leading two-loop electroweak corrections are then of $\mathcal{O}(x_t)$. In the presence of fourth-generation fermions $F = U, D, N, E$, we assume that their masses obey

$$M_Z, M_W, M_{h^0}, M_{H^0}, M_{A^0}, M_{H^\pm} < m_U, m_D, m_N, m_E. \quad (33)$$

For simplicity, we consider the special cases $m_U \gg m_D$, $m_U = m_D$, and $m_U \ll m_D$, and similarly for the leptonic weak-isospin doublet, so that we are effectively dealing with single-scale problems yielding corrections of $\mathcal{O}(x_F)$.

We first list the non-vanishing counterterms entering Eq. (28) for a generic quark doublet (U, D) . For the U quark, we have

$$\frac{\delta m_U}{m_U} = \begin{cases} \frac{x_U}{\sin^2 \beta} \left(\frac{3}{2} \Delta + \frac{3}{2} \ln \frac{\mu^2}{m_U^2} + 4 \right) & \text{if } m_U \gg m_D, \\ x_U \left(\frac{3}{\sin^2 \beta} + \frac{1}{\cos^2 \beta} \right) \left(\frac{1}{2} \Delta + \frac{1}{2} \ln \frac{\mu^2}{m_U^2} + \frac{3}{2} \right) & \text{if } m_U = m_D, \\ \frac{x_D}{\cos^2 \beta} \left(\frac{1}{2} \Delta + \frac{1}{2} \ln \frac{\mu^2}{m_D^2} + \frac{3}{4} \right) & \text{if } m_U \ll m_D. \end{cases} \quad (34)$$

The corresponding expression for the D quark is obtained from Eq. (34) by interchanging $m_U \leftrightarrow m_D$ and $\sin \beta \leftrightarrow \cos \beta$. Furthermore, we have

$$\delta_u = \begin{cases} \frac{N_c}{2} x_U & \text{if } m_U \gg m_D, \\ 0 & \text{if } m_U = m_D, \\ \frac{N_c}{2} x_D & \text{if } m_U \ll m_D. \end{cases} \quad (35)$$

The counterparts of Eqs. (34) and (35) for a generic lepton doublet (N, E) are obtained by substituting $m_U \rightarrow m_N$, $m_D \rightarrow m_E$, and $N_c \rightarrow 1$.

Our final result for the three-generation case reads

$$\mathcal{A}_t^{x_t} = 2^{1/4} G_F^{1/2} \frac{\alpha_{\text{em}}}{\pi} N_c x_t \cot \beta \left(\frac{20}{9} + \frac{6}{9} - \frac{12 \cos^2 \alpha}{9 \sin^2 \beta} - \frac{12 \sin^2 \alpha}{9 \sin^2 \beta} + \frac{20}{9} \cot^2 \beta + \frac{6}{9} \cot^2 \beta - \frac{2}{9} N_c \right) \quad (36)$$

$$= 2^{1/4} G_F^{1/2} \frac{\alpha_{\text{em}}}{\pi} N_c x_t \left[\frac{14}{9} \cot^3 \beta + \frac{2}{9} (7 - N_c) \cot \beta \right], \quad (37)$$

where α is the angle that rotates the weak eigenstates of the neutral CP-even Higgs bosons into their mass eigenstates. On the right-hand side of Eq. (36), we exhibit separately the finite contributions from the χ^0 , ϕ^\pm , h^0 , H^0 , A^0 , and H^\pm bosons, and the universal counterterm, after top-quark mass renormalisation, in the order in which they appear there. The UV-divergent parts vanish after exploiting simple trigonometric identities. The same is true for the unrenormalised contributions from neutral particles as well as for the naïve contributions from the asymptotic expansion of the diagrams containing charged particles. However, the total result is nonzero, as opposed to the QCD case. We observe that the α dependence carried by the contributions from the neutral CP-even Higgs bosons cancels in their sum. This reflects the fact that, by neglecting their masses, we effectively treat the h^0 and H^0 bosons as mass degenerate, so that we may rotate the angle α away.

Now we examine the influence of a sequential generation consisting of heavy fermions F as specified above. Besides the appearance of new leading correction terms quadratic in their masses, of generic order $\mathcal{O}(x_F)$, also the $\mathcal{O}(x_t)$ correction is then modified. This may be understood by observing that the LO result then receives three more mass-independent contributions in addition to the one from the top quark, from the charged fermions U, D, E , which feed into the $\mathcal{O}(x_t)$ correction through the universal counterterm δ_u . This may be accommodated in Eq. (36) through the substitution

$$-\frac{2}{9} N_c \rightarrow -\frac{2}{9} N_c - \frac{2}{9} N_c - \frac{N_c}{18} \tan^2 \beta - \frac{1}{2} \tan^2 \beta. \quad (38)$$

The $\mathcal{O}(x_F)$ contribution due to the (U, D) doublet is found to be

$$\frac{\mathcal{A}_{(U,D)}^{x_F}}{2^{1/4} G_F^{1/2} (\alpha_{\text{em}}/\pi) N_c} = \begin{cases} x_U \left(\frac{4}{3} \cot^3 \beta + \frac{13 - 4N_c}{9} \cot \beta - \frac{7 + N_c}{18} \tan \beta \right) & \text{if } m_U \gg m_D, \\ x_U \left(\frac{4}{3} \cot^3 \beta + \frac{17}{9} \cot \beta + \frac{8}{9} \tan \beta + \frac{1}{3} \tan^3 \beta \right) & \text{if } m_U = m_D, \\ x_D \left[\frac{4}{9} (1 - N_c) \cot \beta + \frac{5 - N_c}{18} \tan \beta + \frac{1}{3} \tan^3 \beta \right] & \text{if } m_U \ll m_D. \end{cases} \quad (39)$$

In each case, we find that the contributions from the various proper two-loop diagrams cancel, so that we are only left with the counterterm contributions. Again, the total result is non-zero, in contrast to the QCD case.

The counterpart of Eq. (39) for the (N, E) doublet is simply obtained by appropriately adjusting the quantum numbers N_f and Q_f and reads:

$$\frac{\mathcal{A}_{(N,E)}^{x_F}}{2^{1/4} G_F^{1/2} (\alpha_{\text{em}}/\pi)} = \begin{cases} x_N \left[\left(1 - \frac{4}{9} N_c \right) \cot \beta + \frac{1}{2} \left(1 - \frac{N_c}{9} \right) \tan \beta \right] & \text{if } m_N \gg m_E, \\ x_N (\cot \beta + 4 \tan \beta + 3 \tan^3 \beta) & \text{if } m_N = m_E, \\ x_E \left[-\frac{4}{9} N_c \cot \beta + \frac{1}{2} \left(5 - \frac{N_c}{9} \right) \tan \beta + 3 \tan^3 \beta \right] & \text{if } m_N \ll m_E. \end{cases} \quad (40)$$

3.3 $\mathcal{O}(x_t)$ and $\mathcal{O}(x_F)$ corrections to $\Gamma(A^0 \rightarrow gg)$

Now we turn to the $\mathcal{O}(x_t)$ and $\mathcal{O}(x_F)$ corrections to $\Gamma(A^0 \rightarrow gg)$. They may be easily extracted from the analogous calculation for $\Gamma(A^0 \rightarrow \gamma\gamma)$ discussed in Section 3.2, by retaining only those diagrams where both photons couple to quark lines and substituting $\alpha_{\text{em}} Q_q Q_{q'} N_c \rightarrow \alpha_s$. Note that this does not affect the factors of N_c originating from the renormalisation procedure.

In the three-generation case, we thus obtain

$$\mathcal{A}_t^{x_t} = 2^{1/4} G_F \frac{\alpha_s}{\pi} x_t \cot \beta \left(5 + 3 - 3 \frac{\cos^2 \alpha}{\sin^2 \beta} - 3 \frac{\sin^2 \alpha}{\sin^2 \beta} + 5 \cot^2 \beta + 3 \cot^2 \beta - \frac{N_c}{2} \right) \quad (41)$$

$$= 2^{1/4} G_F \frac{\alpha_s}{\pi} x_t \left[5 \cot^3 \beta + \left(5 - \frac{N_c}{2} \right) \cot \beta \right], \quad (42)$$

where the five terms on the right-hand side of Eq. (41) again represent the finite contributions from the χ^0 , ϕ^\pm , h^0 , H^0 , A^0 , and H^\pm bosons, and the universal counterterm, after top-quark mass renormalisation. The final result is again independent of α .

In the presence of a sequential heavy-fermion generation, the universal counterterm in Eq. (41) is modified according to

$$-\frac{N_c}{2} \rightarrow -\frac{N_c}{2} - \frac{N_c}{2} - \frac{N_c}{2} \tan^2 \beta. \quad (43)$$

The $\mathcal{O}(x_F)$ contribution due to the (U, D) doublet is found to be

$$\frac{\mathcal{A}_{(U,D)}^{x_F}}{2^{1/4} G_F^{1/2} (\alpha_s/\pi)} = \begin{cases} x_U \left[3 \cot^3 \beta + (4 - N_c) \cot \beta + \left(1 - \frac{N_c}{2}\right) \tan \beta \right] & \text{if } m_U \gg m_D, \\ x_U (3 \cot^3 \beta + 5 \cot \beta + 5 \tan \beta + 3 \tan^3 \beta) & \text{if } m_U = m_D, \\ x_D \left[(1 - N_c) \cot \beta + \left(4 - \frac{N_c}{2}\right) \tan \beta + 3 \tan^3 \beta \right] & \text{if } m_U \ll m_D. \end{cases} \quad (44)$$

The (N, E) doublet can generate a $\mathcal{O}(x_F)$ contribution only through the universal counterterm, so that

$$\frac{\mathcal{A}_{(N,E)}^{x_F}}{2^{1/4} G_F^{1/2} (\alpha_s/\pi)} = \begin{cases} x_N \left(-\cot \beta - \frac{1}{2} \tan \beta \right) & \text{if } m_N \gg m_E, \\ 0 & \text{if } m_N = m_E, \\ x_E \left(-\cot \beta - \frac{1}{2} \tan \beta \right) & \text{if } m_N \ll m_E. \end{cases} \quad (45)$$

Note that the $\mathcal{O}(\alpha_s)$ correction to $\Gamma(A^0 \rightarrow gg)$ cannot be recovered from the one to $\Gamma(A^0 \rightarrow \gamma\gamma)$ because it receives additional contributions from diagrams involving gluon self-couplings.

4 $\mathcal{O}(x_f)$ correction to $\Gamma(H \rightarrow \gamma\gamma)$

Applying similar techniques as in Section 3.2, we now also derive the $\mathcal{O}(x_f)$ correction to $\Gamma(H \rightarrow \gamma\gamma)$ in the SM endowed with a sequential generation of heavy fermions. Due to electromagnetic gauge invariance, the transition-matrix element of $H \rightarrow \gamma\gamma$ possesses the structure

$$\mathcal{T} = [(q_1 \cdot q_2) g^{\mu\nu} - q_1^\nu q_2^\mu] \epsilon_\mu^*(q_1) \epsilon_\nu^*(q_2) \mathcal{A}. \quad (46)$$

To obtain a strong check on our analysis, we actually verify electromagnetic gauge invariance by separately projecting out the coefficients of the Lorentz tensors $(q_1 \cdot q_2) g^{\mu\nu}$ and $q_1^\nu q_2^\mu$ in Eq. (46). Furthermore, we work in general R_ξ gauge, so as to verify that the gauge parameter ξ cancels in the final result. From Eq. (46), we obtain

$$\Gamma(H \rightarrow \gamma\gamma) = \frac{M_H^3}{64\pi} |\mathcal{A}|^2, \quad (47)$$

where M_H is the mass of the SM Higgs boson.

The form factor \mathcal{A} is evaluated in perturbation theory as

$$\mathcal{A} = \mathcal{A}_W^{\text{LO}} + \sum_f (\mathcal{A}_f^{\text{LO}} + \mathcal{A}_f^{\alpha_s} + \mathcal{A}_f^{x_f} + \dots) + \dots, \quad (48)$$

where $\mathcal{A}_W^{\text{LO}}$ denotes the one-loop contribution due to the W^\pm boson and the other contributions carry similar meanings as in Eq. (23).

A comprehensive review of the present theoretical knowledge of $\Gamma(H \rightarrow \gamma\gamma)$ may be found in Ref. [40]. The LO result was first obtained in Ref. [41]. The $\mathcal{O}(\alpha_s)$ [12,42] and $\mathcal{O}(\alpha_s^2)$ [43] QCD corrections are also available. As for the two-loop electroweak correction, the contributions induced by light [44] and heavy fermions [20,45] as well as the residual ones [46] were recently evaluated. The $\mathcal{O}(x_F)$ correction due to a sequential generation of heavy fermions was studied in Ref. [20] for general values of their masses. In the following, we revisit this analysis for the mass hierarchies $m_U \gg m_D$, $m_U = m_D$, and $m_U \ll m_D$, and similarly for the leptons N and E using asymptotic expansion. We refrain from considering $\Gamma(H \rightarrow gg)$.

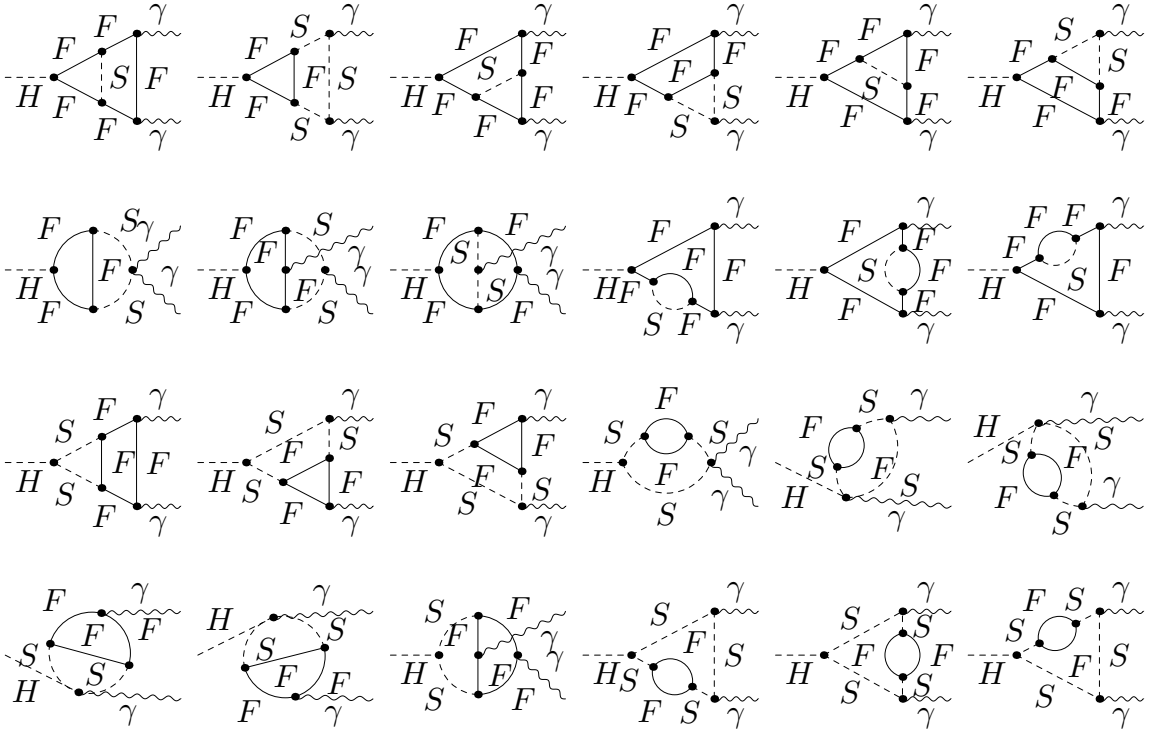


Figure 6: Generic two-loop diagrams contributing to the $\mathcal{O}(x_F)$ electroweak correction to $\Gamma(H \rightarrow \gamma\gamma)$. $S = \chi^0, \phi^\pm, W^\pm, H$ and $F = U, D, N, E$ denote generic bosons and fermions, respectively. The couplings of the neutral particles to the photon vanish.

The diagrams contributing to $\Gamma(H \rightarrow \gamma\gamma)$ at $\mathcal{O}(x_F)$ are shown generically in Fig. 6. In contrast to the case of $A^0 \rightarrow \gamma\gamma$, now also virtual W^\pm bosons participate in $\mathcal{O}(x_F)$ [20,45].

Unlike in Refs. [47,48], we choose not to perform tadpole renormalisation here. In turn, we need to include the diagrams that are generated by attaching a Higgs tadpole in all possible ways to any one-loop seed diagram. Some examples are depicted in Fig. 7. These tadpole diagrams yield terms proportional to m_F^4 , which cancel against the tadpole contributions to the counterterms, which are all proportional to m_F^4 , and the m_F^4

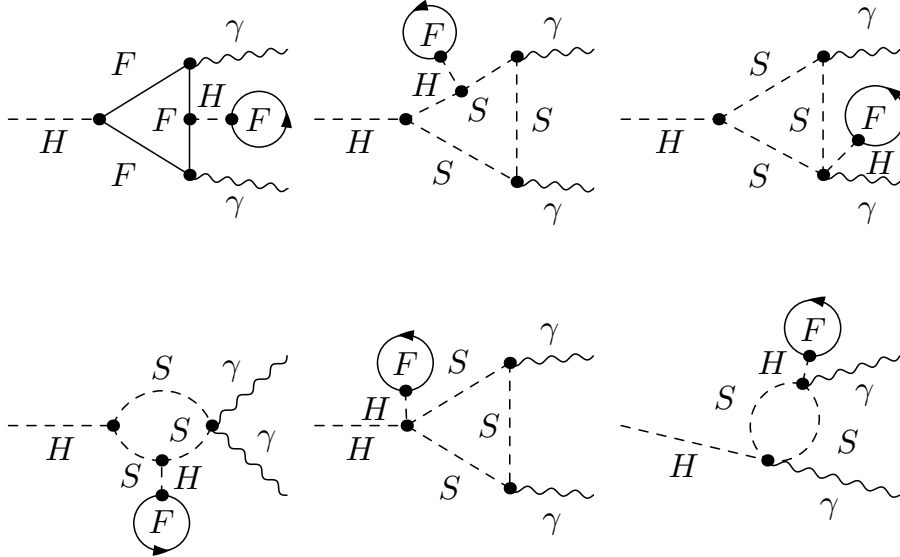


Figure 7: Examples of two-loop tadpole diagrams contributing to the $\mathcal{O}(x_F)$ electroweak correction to $\Gamma(H \rightarrow \gamma\gamma)$. $S = \chi^0, \phi^\pm, W^\pm, H$ and $F = U, D, N, E$ denote generic bosons and fermions, respectively. The couplings of the neutral particles to the photon vanish.

terms from the Higgs mass renormalisation and the asymptotic expansion of the two-loop diagrams involving virtual ϕ^\pm bosons. Thus, the final result is devoid of m_F^4 terms.

It is interesting to note that the contribution from the attachment of a tadpole to a fermion line is cancelled by the m_F^4 term from the renormalisation of the mass of that line in the one-loop seed diagram. Furthermore, the tadpole contributions to the renormalisations of the factors $1/M_W$ and m_F in the $H F \bar{F}$ vertex cancel each other. These are the only tadpole contributions that could generate m_F^2 terms in the final result, through the expansion in τ_F .

Prior to evaluating the proper diagrams of Figs. 6 and 7, we discuss the renormalisation in some detail. As before, we need to renormalise the Higgs-boson wave function and the masses of the W^\pm boson and the heavy fermions. In addition, we now also need to renormalise the Higgs-boson mass. The parameter M_W appears in the W^\pm, ϕ^\pm , and u^\pm propagators and in the $H W^\pm W^\mp, H \phi^\pm W^\mp, \phi^\pm W^\mp \gamma, H \phi^\pm W^\mp \gamma$, and $H F \bar{F}$ vertices, where u^\pm are the charged Faddeev-Popov ghosts. The only vertex involving M_H is $H \phi^\pm \phi^\mp$, which induces two-loop contributions via δM_H . Finally, m_F occurs in the F -fermion propagator and in the $H F \bar{F}$ vertex. The corresponding counterterms are defined through

$$\begin{aligned}
m_F^0 &= m_F + \delta m_F + \delta m_F^{\text{tad}}, \\
(M_W^0)^2 &= M_W^2 + \delta M_W^2 + \delta M_W^{2,\text{tad}}, \\
(M_H^0)^2 &= M_H^2 + \delta M_H^2 + \delta M_H^{2,\text{tad}}, \\
H^0 &= \sqrt{Z_H} H = \left(1 + \frac{1}{2} \delta Z_H\right) H,
\end{aligned} \tag{49}$$

where tadpole contributions are marked by the superscript “tad.” Note that δZ_H is obtained from the derivative of the Higgs-boson self-energy and thus has no tadpole contribution.

In the case of the (U, D) doublet, the counterterms in Eq. (49) read:

$$\begin{aligned}
\frac{\delta m_U}{m_U} &= \begin{cases} x_U \left(\frac{3}{2}\Delta + \frac{3}{2} \ln \frac{\mu^2}{m_U^2} + 4 \right) & \text{if } m_U \gg m_D, \\ 2x_U & \text{if } m_U = m_D, \\ x_D \left(-\frac{3}{2}\Delta - \frac{3}{2} \ln \frac{\mu^2}{m_D^2} - \frac{5}{4} \right) & \text{if } m_U \ll m_D, \end{cases} \\
\frac{\delta m_U^{\text{tad}}}{m_U} &= \begin{cases} x_U N_c \frac{m_U^2}{M_H^2} \left(4\Delta + 4 \ln \frac{\mu^2}{m_U^2} + 4 \right) & \text{if } m_U \gg m_D, \\ x_U N_c \frac{m_U^2}{M_H^2} \left(8\Delta + 8 \ln \frac{\mu^2}{m_U^2} + 8 \right) & \text{if } m_U = m_D, \\ x_D N_c \frac{m_D^2}{M_H^2} \left(4\Delta + 4 \ln \frac{\mu^2}{m_D^2} + 4 \right) & \text{if } m_U \ll m_D, \end{cases} \\
\frac{\delta M_W^2}{M_W^2} &= \begin{cases} x_U N_c \left(-2\Delta - 2 \ln \frac{\mu^2}{m_U^2} - 1 \right) & \text{if } m_U \gg m_D, \\ x_U N_c \left(-4\Delta - 4 \ln \frac{\mu^2}{m_U^2} \right) & \text{if } m_U = m_D, \\ x_D N_c \left(-2\Delta - 2 \ln \frac{\mu^2}{m_D^2} - 1 \right) & \text{if } m_U \ll m_D, \end{cases} \\
\frac{\delta M_W^{2,\text{tad}}}{M_W^2} &= 2 \frac{\delta m_U^{\text{tad}}}{m_U}, \\
\frac{\delta M_H^2}{M_H^2} &= \begin{cases} x_U N_c \left[\frac{m_U^2}{M_H^2} \left(-12\Delta - 12 \ln \frac{\mu^2}{m_U^2} - 4 \right) + 2\Delta + 2 \ln \frac{\mu^2}{m_U^2} - \frac{4}{3} \right] & \text{if } m_U \gg m_D, \\ x_U N_c \left[\frac{m_U^2}{M_H^2} \left(-24\Delta - 24 \ln \frac{\mu^2}{m_U^2} - 8 \right) + 4\Delta + 4 \ln \frac{\mu^2}{m_U^2} - \frac{8}{3} \right] & \text{if } m_U = m_D, \\ x_D N_c \left[\frac{m_D^2}{M_H^2} \left(-12\Delta - 12 \ln \frac{\mu^2}{m_D^2} - 4 \right) + 2\Delta + 2 \ln \frac{\mu^2}{m_D^2} - \frac{4}{3} \right] & \text{if } m_U \ll m_D, \end{cases} \\
\frac{\delta M_H^{2,\text{tad}}}{M_H^2} &= 3 \frac{\delta m_U^{\text{tad}}}{m_U}, \\
\delta Z_H &= \begin{cases} x_U N_c \left(-2\Delta - 2 \ln \frac{\mu^2}{m_U^2} + \frac{4}{3} \right) & \text{if } m_U \gg m_D, \\ x_U N_c \left(-4\Delta - 4 \ln \frac{\mu^2}{m_U^2} + \frac{8}{3} \right) & \text{if } m_U = m_D, \\ x_D N_c \left(-2\Delta - 2 \ln \frac{\mu^2}{m_D^2} + \frac{4}{3} \right) & \text{if } m_U \ll m_D, \end{cases} \quad (50)
\end{aligned}$$

and similarly for $\delta m_D/m_D$ and $\delta m_D^{\text{tad}}/m_D$. The renormalisations of the Higgs-boson wave function and the W -boson mass in the $H\overline{F}F$ Yukawa coupling combine to a universal

correction [49],

$$\delta_u = \frac{1}{2} \left(\delta Z_H - \frac{\delta M_W^2}{M_W^2} \right), \quad (51)$$

which should be compared with Eq. (30) for the case of the A^0 boson. We have [50]

$$\delta_u = \begin{cases} \frac{7}{6} x_U N_c & \text{if } m_U \gg m_D, \\ \frac{4}{3} x_U N_c & \text{if } m_U = m_D, \\ \frac{7}{6} x_D N_c & \text{if } m_U \ll m_D. \end{cases} \quad (52)$$

The counterparts of Eqs. (50) and (52) for the (N, E) doublet are obtained by substituting $m_U \rightarrow m_N$, $m_D \rightarrow m_E$, and $N_c \rightarrow 1$. Those for the three-generation SM may be found in Eqs. (68)–(71), (74)–(76), and (80) of Ref. [48].

We now list our final results for $\mathcal{A}_f^{x_f}$ due to the (U, D) doublet. For the sake of comparison with Ref. [20], we exhibit the dependence on the electric charge of the heavier quark, exploiting the relation $Q_U = Q_D + 1$. We find

$$\begin{aligned} \frac{\mathcal{A}_{(U,D)}^{x_F}}{2^{1/4} G_F^{1/2} (\alpha_{\text{em}}/\pi) N_c} &= \begin{cases} x_U \left[-\frac{25}{36} - 6Q_U + 4Q_U^2 - \frac{7}{9} N_c (1 - 2Q_U + 3Q_U^2) \right] & \text{if } m_U \gg m_D, \\ x_U \left[-\frac{56}{9} - 8Q_U + 8Q_U^2 - \frac{8}{9} N_c (1 - 2Q_U + 3Q_U^2) \right] & \text{if } m_U = m_D, \\ x_D \left[-\frac{25}{36} + 6Q_D + 4Q_D^2 - \frac{7}{9} N_c (2 + 4Q_D + 3Q_D^2) \right] & \text{if } m_U \ll m_D, \end{cases} \\ &= \begin{cases} x_U \left(-\frac{35}{12} - \frac{7}{9} N_c \right) & \text{if } m_U \gg m_D, \\ x_U \left(-8 - \frac{8}{9} N_c \right) & \text{if } m_U = m_D, \\ x_D \left(-\frac{9}{4} - \frac{7}{9} N_c \right) & \text{if } m_U \ll m_D. \end{cases} \end{aligned} \quad (53)$$

Appropriately adjusting the quantum numbers in the various contributions, we find $\mathcal{A}_f^{x_f}$ due to the (N, E) doublet to be

$$\frac{\mathcal{A}_{(N,E)}^{x_F}}{2^{1/4} G_F^{1/2} (\alpha_{\text{em}}/\pi)} = \begin{cases} x_N \left(-\frac{25}{36} - \frac{7}{9} N_c \right) & \text{if } m_N \gg m_E, \\ x_N \left(-\frac{56}{9} - \frac{8}{9} N_c \right) & \text{if } m_N = m_E, \\ x_E \left(-\frac{97}{36} - \frac{7}{9} N_c \right) & \text{if } m_N \ll m_E. \end{cases} \quad (54)$$

In the remainder of this section, we compare our results with those obtained in Ref. [20]. That reference is more general than ours in the sense that no hierarchies

among the heavy-fermion masses are assumed. However, we can compare Eq. (53) with Eqs. (56) and (57) of Ref. [20], where the hierarchies $m_U \gg m_D$ and $m_U = m_D$, respectively, are considered. We can reproduce these equations if we include an overall minus sign in our expression for $\delta m_U/m_U$ in Eq. (50). In other words, there should be an overall minus sign on the right-hand side of Eq. (9) in Ref. [20], which was already noticed in Ref. [45] in connection with the SM case. In Ref. [45], it was also observed that the limit $m_D \rightarrow 0$ of the fourth-generation result for $M_W \ll m_D \ll m_U$ differs from the calculation with $m_D = 0$ from the beginning, which is appropriate for the third generation, where $m_b \ll M_W \ll m_t$. These two observations lead to a modification of Eq. (60) in Ref. [20], where the leading correction due to the five heavy fermions t, U, D, N , and E is presented. Adopting the notation of Ref. [20], we have

$$A_{4\text{gen}} = \frac{\alpha G_\mu^{1/2}}{\pi 2^{3/4}} \frac{5}{3} \left[1 + \frac{G_\mu}{8\pi^2 \sqrt{2}} \left(-\frac{197}{10} m_t^2 - \frac{109}{30} m_N^2 - \frac{181}{30} m_E^2 - \frac{m_N^2 m_E^2}{m_N^2 - m_E^2} \ln \frac{m_N^2}{m_E^2} - \frac{189}{10} m_U^2 - \frac{33}{2} m_D^2 - 3 \frac{m_U^2 m_D^2}{m_U^2 - m_D^2} \ln \frac{m_U^2}{m_D^2} \right) \right], \quad (55)$$

where $\alpha = \alpha_{\text{em}}$ and $G_\mu = G_F$. By the same token, Eq. (59) of Ref. [20] becomes [45,46]:

$$A_{\text{SM}} = \frac{\alpha G_\mu^{1/2}}{\pi 2^{3/4}} \frac{47}{9} \left[1 + \frac{G_\mu}{8\pi^2 \sqrt{2}} \left(-\frac{367}{94} m_t^2 \right) \right]. \quad (56)$$

In Ref. [20], the $\mathcal{O}(x_f)$ corrections to the Hgg coupling in the SM with and without a sequential generation of heavy fermions were inferred from those $H\gamma\gamma$ diagrams where the photons are directly coupled to loop quarks. In the case of the $\mathcal{O}(x_t)$ corrections, the effects due to the flipped sign in the top-quark mass counterterm and the interchange of mass limits in the proper diagrams incidentally compensate each other, so that Eq. (61) in Ref. [20] agrees with Refs. [45,51]. In the case of the $\mathcal{O}(x_F)$ corrections, where no mass limits are interchanged, the fermion mass counterterms cancel within each isodoublet, so that Eq. (62) of Ref. [20] goes unchanged.

5 Discussion

We now explore the phenomenological implications of our results for $\Gamma(A^0 \rightarrow \gamma\gamma)$ and $\Gamma(A^0 \rightarrow gg)$. For definiteness, we concentrate on the more likely case of three generations. As explained in Section 1, we consider a scenario with low to intermediate values of the Higgs-boson masses and $\tan\beta$ and large values of the supersymmetric-particle masses, so that the dominant electroweak two-loop corrections are of relative order $\mathcal{O}(x_t)$. We adopt the following values for our input parameters [31]: $G_F = 1.16637 \times 10^{-5} \text{ GeV}^{-2}$, $\alpha_s(M_Z) = 0.1176$, and $m_t = 170.9 \text{ GeV}$. As for the unknown 2HDM input parameters, we assume that $M_{A^0} < 160 \text{ GeV}$ and $2 < \tan\beta < 10$. For larger values of $\tan\beta$, our approximation of neglecting the bottom-quark contributions is likely to break down.

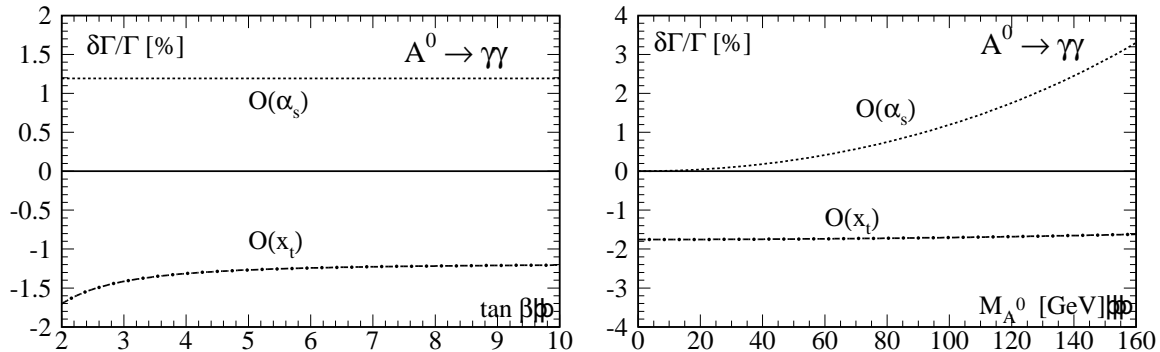


Figure 8: $\mathcal{O}(x_t)$ and $\mathcal{O}(\alpha_s)$ corrections to $\Gamma(A^0 \rightarrow \gamma\gamma)$ (a) for $M_{A^0} = 100$ GeV as functions of $\tan\beta$ and (b) for $\tan\beta = 2$ as functions of M_{A^0} .

We first consider $\Gamma(A^0 \rightarrow \gamma\gamma)$. Neglecting the bottom-quark contribution, its $\mathcal{O}(x_t)$ correction is given by

$$\begin{aligned} \frac{\delta\Gamma}{\Gamma} &= 2 \frac{\mathcal{A}_t^{x_f}}{\mathcal{A}_t^{\text{LO}}} \\ &= -x_t \left[4 + \frac{7}{\tan^2\beta} + \mathcal{O}(\tau_t) \right], \end{aligned} \quad (57)$$

where, in the second equality, $\mathcal{A}_t^{\text{LO}}$ is approximated by the leading term in the second line of Eq. (24) for $f = t$. We observe that this correction is negative, has its maximum size for small values of $\tan\beta$, and is independent of M_{A^0} , apart from the M_{A^0} dependence carried by $\mathcal{A}_t^{\text{LO}}$. Its evaluation according to the first line of Eq. (57) is compared with the $\mathcal{O}(\alpha_s)$ correction in Fig. 8. We observe from Fig. 8(a) that the $\mathcal{O}(x_t)$ correction amounts to -1.7% at $\tan\beta = 2$ and rapidly reaches its asymptotic value of -1.2% as $\tan\beta$ increases, whereas the $\mathcal{O}(\alpha_s)$ correction, evaluated from Eqs. (24) and (27), is positive and independent of $\tan\beta$, as long as the bottom-quark contribution is neglected. The M_{A^0} dependence of the $\mathcal{O}(x_t)$ correction shown in Fig. 8(b), which is induced by $\mathcal{A}_t^{\text{LO}}$ as mentioned above, is rather feeble, so that we may expect the unknown $\mathcal{O}(\tau_t^n)$ ($n = 1, 2, 3, \dots$) terms in Eq. (57) to be of moderate size, too. The smallness and approximately quadratic M_{A^0} dependence of the $\mathcal{O}(\alpha_s)$ correction is due to the absence of the leading $\mathcal{O}(\tau_t^0)$ term in $\mathcal{A}_t^{\alpha_s}$, given by Eq. (27). We conclude that the $\mathcal{O}(x_t)$ reduction more than compensates the $\mathcal{O}(\alpha_s)$ enhancement for $M_{A^0} \lesssim 120$ GeV.

We now turn to $\Gamma(A^0 \rightarrow gg)$. For $\tau_t \ll 1$, its $\mathcal{O}(x_t)$ correction reads

$$\begin{aligned} \frac{\delta\Gamma}{\Gamma} &= 2 \frac{\mathcal{A}_t^{x_f}}{\mathcal{A}_t^{\text{LO}}} \\ &= -x_t \left[7 + \frac{10}{\tan^2\beta} + \mathcal{O}(\tau_t) \right]. \end{aligned} \quad (58)$$

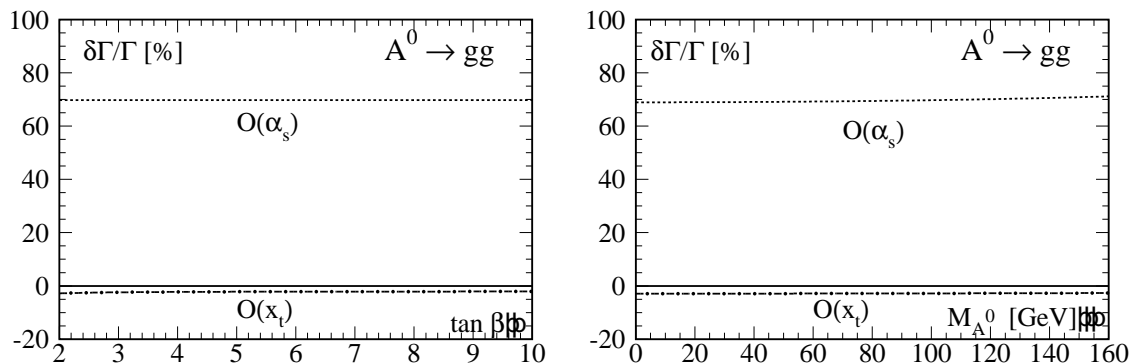


Figure 9: $\mathcal{O}(x_t)$ and $\mathcal{O}(\alpha_s)$ corrections to $\Gamma(A^0 \rightarrow gg)$ (a) for $M_{A^0} = 100$ GeV as functions of $\tan\beta$ and (b) for $\tan\beta = 2$ as functions of M_{A^0} .

As in the case of $A^0 \rightarrow \gamma\gamma$, this correction is negative, has its maximum size for small values of $\tan\beta$, and is independent of M_{A^0} , apart from the M_{A^0} dependence carried by $\mathcal{A}_t^{\text{LO}}$. In Fig. 9, its evaluation according to the first line of Eq. (58) is compared with the full $\mathcal{O}(\alpha_s)$ correction [10] due to virtual top quarks, which also involves three-parton final states. In contrast to the case of $A^0 \rightarrow \gamma\gamma$, the $\mathcal{O}(\alpha_s)$ correction to $\Gamma(A^0 \rightarrow gg)$ does have a $\mathcal{O}(\tau_t^0)$ term, which is about 68%. The $\mathcal{O}(\tau_t^0)$ term is also known at $\mathcal{O}(\alpha_s^2)$, where it is still as large as 23% [16]. The $\mathcal{O}(x_t)$ correction to $\Gamma(A^0 \rightarrow gg)$ ranges from -2.8% at $\tan\beta = 2$ to the asymptotic value -2.1% and partly screens the sizeable $\mathcal{O}(\alpha_s)$ and $\mathcal{O}(\alpha_s^2)$ corrections.

Let us now briefly comment on the $\mathcal{O}(x_F)$ corrections to $\Gamma(A^0 \rightarrow \gamma\gamma)$ and $\Gamma(A^0 \rightarrow gg)$ due to a sequential generation of heavy fermions, given in Eqs. (39), (40), (44), and (45). These can be sizeable for large values of m_F just because of the prefactor x_F . For large values of $\tan\beta$, further enhancement comes from the terms of maximum power in $\tan\beta$, which are cubic for $m_U \approx m_D$, $m_U \ll m_D$, $m_N \approx m_E$, and $m_N \ll m_E$ in the case of $A^0 \rightarrow \gamma\gamma$ and for $m_U \approx m_D$ and $m_U \ll m_D$ in the case of $A^0 \rightarrow gg$, and (at most) linear for the other mass hierarchies. For $\tan\beta > 2$, the $\mathcal{O}(x_F)$ corrections reduce the LO results for $\Gamma(A^0 \rightarrow \gamma\gamma)$ and $\Gamma(A^0 \rightarrow gg)$, except for the corrections due to a (U, D) doublet with $m_U \gg m_D$ and, in the case of $\Gamma(A^0 \rightarrow gg)$, also those due to the (N, E) doublet. Because of the constraint from electroweak precision tests [31] on the rho parameter [20,52], the case of approximate mass degeneracy within the (U, D) and (N, E) doublets is favoured, so that a $\tan^3\beta$ -enhanced screening is likely to be encountered.

6 Conclusions

In conclusion, we analytically calculated the dominant electroweak two-loop corrections, of order $\mathcal{O}(x_t)$, to $\Gamma(A^0 \rightarrow \gamma\gamma)$, $\Gamma(A^0 \rightarrow gg)$, $\sigma(\gamma\gamma \rightarrow A^0)$, and $\sigma(gg \rightarrow A^0)$ within the 2HDM with low- to intermediate-mass Higgs bosons for small to moderate value of $\tan\beta$ using asymptotic expansion in $M_{A^0}^2/(2m_t)^2$. We also studied how these corrections are

modified by the presence of a sequential generation of heavy fermions, with generic mass m_F , and provided the $\mathcal{O}(x_F)$ corrections arising then in addition. We also revisited the $\mathcal{O}(x_t)$ and $\mathcal{O}(x_F)$ corrections to $\Gamma(H \rightarrow \gamma\gamma)$ and $\sigma(\gamma\gamma \rightarrow H)$ in the four-generation SM and clarified an inconsistency in Ref. [20].

We recovered the notion that the naïve treatment of the γ_5 matrix being anticommuting in d space-time dimensions leads to ambiguous results, which depend on the way of executing the Dirac traces. To consistently overcome the non-trivial γ_5 problem of dimensional regularisation, we adopted the HVBM scheme [21] and included a finite renormalisation constant, Z_5^p , for the pseudoscalar current to effectively restore the anti-commutativity of the γ_5 matrix [22,23,24]. The $\mathcal{O}(x_t)$ and $\mathcal{O}(x_F)$ terms of Z_5^p were found to vanish. We worked in the electroweak on-shell renormalisation scheme [32,33] endowed with the DCPR definition of $\tan\beta$ [35,36].

On the phenomenological side, the $\mathcal{O}(x_t)$ correction to $\Gamma(A^0 \rightarrow \gamma\gamma)$ and $\sigma(\gamma\gamma \rightarrow A^0)$ is of relative importance, since it more than compensates the $\mathcal{O}(\alpha_s)$ enhancement for $M_{A^0} \lesssim 120$ GeV. It leads to a reduction of the LO results, which ranges between -1.7% and -1.2% for $2 < \tan\beta < 10$ and is independent of M_{A^0} . Such an effect might be measurable for $\sigma(\gamma\gamma \rightarrow A^0)$ at the ILC operated in the $\gamma\gamma$ mode on the A^0 -boson resonance and possibly also for $\Gamma(A^0 \rightarrow \gamma\gamma)$ at the ILC in the regular e^+e^- mode [7].

As for $\Gamma(A^0 \rightarrow gg)$ and $\sigma(gg \rightarrow A^0)$, the $\mathcal{O}(x_t)$ correction screens the sizeable QCD enhancement, by between -2.8% and -2.1% for $2 < \tan\beta < 10$, and is independent of M_{A^0} . Such a reduction of $\sigma(gg \rightarrow A^0)$ should matter at the high luminosities to be achieved at the LHC. E.g., given an annual luminosity of 100 fb^{-1} per LHC experiment, a $pp \rightarrow A^0 + X$ cross section of about 35 pb (for $M_{A^0} = 100$ GeV and $\tan\beta = 2$) [3] amounts to 7×10^6 A^0 bosons per year, 2.8% of which still corresponds to a substantial subsample of 200.000 A^0 bosons per year. Furthermore, the size of this correction is in the ballpark of the theoretical uncertainty due to the parton distribution functions [10] and the scale dependence of the NNLO QCD prediction [17].

Acknowledgements

We would like to thank M. Gorbahn for helpful discussions, W. Hollik for a useful communication concerning the renormalisation of $\tan\beta$, P. Kant for providing us with the series expansion of the analytic result for the $\mathcal{O}(\alpha_s)$ correction to $\Gamma(A^0 \rightarrow \gamma\gamma)$ in Eq. (2.20) of Ref. [12], M. Spira for providing us with the numerical results for the full $\mathcal{O}(\alpha_s)$ correction to $\Gamma(A^0 \rightarrow gg)$ [10] shown in Fig. 9, and M. Steinhauser for providing us with an updated version of MATAD [28]. This work was supported in part by BMBF Grant No. 05 HT6GUA and DFG Grant No. GRK 602.

References

- [1] F. Gianotti, et al., Eur. Phys. J. C 39 (2005) 293 [arXiv:hep-ph/0204087].

- [2] M. Spira, Fortsch. Phys. 46 (1998) 203 [arXiv:hep-ph/9705337];
M.S. Carena, H.E. Haber, Prog. Part. Nucl. Phys. 50 (2003) 63
[arXiv:hep-ph/0208209].
- [3] A. Djouadi, Phys. Rept. 459 (2008) 1 [arXiv:hep-ph/0503173].
- [4] M.M. Mühlleitner, M. Krämer, M. Spira, P.M. Zerwas, Phys. Lett. B 508 (2001) 311
[arXiv:hep-ph/0101083];
D.M. Asner, J.B. Gronberg, J.F. Gunion, Phys. Rev. D 67 (2003) 035009
[arXiv:hep-ph/0110320];
P. Niezurawski, A.F. Zarnecki, M. Krawczyk, Acta Phys. Polon. B 37 (2006) 1187.
- [5] P. Kalyniak, R. Bates, J.N. Ng, Phys. Rev. D 33 (1986) 755;
R. Bates, J.N. Ng, P. Kalyniak, Phys. Rev. D 34 (1986) 172;
J.F. Gunion, G. Gamberini, S.F. Novaes, Phys. Rev. D 38 (1988) 3481.
- [6] J.F. Gunion, H.E. Haber, Nucl. Phys. B 278 (1986) 449;
J.F. Gunion, H.E. Haber, Nucl. Phys. B 402 (1993) 569, Erratum.
- [7] M. Battaglia, K. Desch, AIP Conf. Proc. 578 (2001) 163 [arXiv:hep-ph/0101165];
A. Droll, H.E. Logan, Phys. Rev. D 76 (2007) 015001 [arXiv:hep-ph/0612317].
- [8] LHC/LC Study Group, G. Weiglein, et al., Phys. Rept. 426 (2006) 47
[arXiv:hep-ph/0410364].
- [9] A. Djouadi, M. Spira, P.M. Zerwas, Phys. Lett. B 311 (1993) 255
[arXiv:hep-ph/9305335].
- [10] M. Spira, A. Djouadi, D. Graudenz, P.M. Zerwas, Nucl. Phys. B 453 (1995) 17
[arXiv:hep-ph/9504378].
- [11] M. Spira, A. Djouadi, D. Graudenz, P.M. Zerwas, Phys. Lett. B 318 (1993) 347.
- [12] R. Harlander, P. Kant, JHEP 0512 (2005) 015 [arXiv:hep-ph/0509189].
- [13] U. Aglietti, R. Bonciani, G. Degrossi, A. Vicini, JHEP 0701 (2007) 021
[arXiv:hep-ph/0611266].
- [14] V. Ravindran, J. Smith, W.L. van Neerven, Nucl. Phys. B 704 (2005) 332
[arXiv:hep-ph/0408315].
- [15] R.P. Kauffman, W. Schaffer, Phys. Rev. D 49 (1994) 551 [arXiv:hep-ph/9305279].
- [16] K.G. Chetyrkin, B.A. Kniehl, M. Steinhauser, W.A. Bardeen, Nucl. Phys. B 535
(1998) 3 [arXiv:hep-ph/9807241].
- [17] R.V. Harlander, W.B. Kilgore, JHEP 0210 (2002) 017 [arXiv:hep-ph/0208096];
C. Anastasiou, K. Melnikov, Phys. Rev. D 67 (2003) 037501 [arXiv:hep-ph/0208115].

- [18] R.V. Harlander, F. Hofmann, JHEP 0603 (2006) 050 [arXiv:hep-ph/0507041].
- [19] J. Brod, F. Fugel, B.A. Kniehl, Report No. DESY 08-010, TTP08-05, and SFB/CPP-08-10 [arXiv:0802.0171 [hep-ph]], accepted for publication in Phys. Rev. D (Rapid Communications).
- [20] A. Djouadi, P. Gambino, B.A. Kniehl, Nucl. Phys. B 523 (1998) 17 [arXiv:hep-ph/9712330].
- [21] G. 't Hooft, M. Veltman, Nucl. Phys. B44 (1972) 189;
P. Breitenlohner, D. Maison, Commun. Math. Phys. 52 (1977) 11.
- [22] T.L. Trueman, Phys. Lett. 88B (1979) 331.
- [23] J.C. Collins, Renormalization, Cambridge University Press, Cambridge, 1984.
- [24] S.A. Larin, Phys. Lett. B 303 (1993) 113 [arXiv:hep-ph/9302240].
- [25] V.A. Smirnov, Applied Asymptotic Expansions in Momenta and Masses, Springer-Verlag, Berlin-Heidelberg, 2001.
- [26] P. Nogueira, J. Comput. Phys. 105 (1993) 279.
- [27] R. Harlander, T. Seidensticker, M. Steinhauser, Phys. Lett. B 426 (1998) 125 [arXiv:hep-ph/9712228];
T. Seidensticker, in: G. Athanasiou (Ed.), Proceedings of the 6th International Workshop on New Computing Techniques in Physics Research: Software Engineering, Artificial Intelligence, Neural Nets, Genetic Algorithms, Symbolic Algebra, Automatic Calculation (AIHENP'99), Heraklion, Greece, 12-16 April 1999, SPIRES Conference No C99/04/12 [arXiv:hep-ph/9905298].
- [28] M. Steinhauser, Comput. Phys. Commun. 134 (2001) 335 [arXiv:hep-ph/0009029].
- [29] J.A.M. Vermaseren, Symbolic Manipulation with FORM, Computer Algebra Netherlands, Amsterdam, 1991.
- [30] W. Hollik, D. Stöckinger, Eur. Phys. J. C 20 (2001) 105 [arXiv:hep-ph/0103009];
I. Fischer, W. Hollik, M. Roth, D. Stöckinger, Phys. Rev. D 69 (2004) 015004 [arXiv:hep-ph/0310191].
- [31] Particle Data Group, W.M. Yao, et al., J. Phys. G 33 (2006) 1 and 2007 partial update for 2008.
- [32] A. Sirlin, Phys. Rev. D 22 (1980) 971.
- [33] W. Hollik, E. Kraus, M. Roth, C. Rupp, K. Sibold, D. Stöckinger, Nucl. Phys. B 639 (2002) 3 [arXiv:hep-ph/0204350].

- [34] A. Freitas, D. Stöckinger, *Phys. Rev. D* 66 (2002) 095014 [arXiv:hep-ph/0205281].
- [35] P.H. Chankowski, S. Pokorski, J. Rosiek, *Nucl. Phys. B* 423 (1994) 437 [arXiv:hep-ph/9303309];
A. Dabelstein, *Z. Phys. C* 67 (1995) 495 [arXiv:hep-ph/9409375].
- [36] A. Dabelstein, *Nucl. Phys. B* 456 (1995) 25 [arXiv:hep-ph/9503443].
- [37] M. Jamin, M.E. Lautenbacher, *Comput. Phys. Commun.* 74 (1993) 265.
- [38] S.L. Adler and W.A. Bardeen, *Phys. Rev.* 182 (1969) 1517.
- [39] B.A. Kniehl, M. Spira, *Z. Phys. C* 69 (1995) 77 [arXiv:hep-ph/9505225].
- [40] B.A. Kniehl, *Phys. Rept.* 240 (1994) 211;
B.A. Kniehl, *Int. J. Mod. Phys. A* 17 (2002) 1457 [arXiv:hep-ph/0112023];
F. Fugel, *Acta Phys. Polon. B* 38 (2007) 761 [arXiv:hep-ph/0608303];
A. Djouadi, *Phys. Rept.* 457 (2008) 1 [arXiv:hep-ph/0503172].
- [41] J.R. Ellis, M.K. Gaillard, D.V. Nanopoulos, *Nucl. Phys. B* 106 (1976) 292;
B.L. Ioffe, V.A. Khoze, *Fiz. Elem. Chastits At. Yadra* 9 (1978) 118 [*Sov. J. Part. Nucl.* 9 (1978) 50];
A.I. Vainshtein, M.B. Voloshin, V.I. Zakharov, M.A. Shifman, *Yad. Fiz.* 30 (1979) 1368 [*Sov. J. Nucl. Phys.* 30 (1979) 711].
- [42] H. Zheng, D. Wu, *Phys. Rev. D* 42 (1990) 3760;
A. Djouadi, M. Spira, J.J. van der Bij, P.M. Zerwas, *Phys. Lett. B* 257 (1991) 187;
S. Dawson, R.P. Kauffman, *Phys. Rev. D* 47 (1993) 1264;
A. Djouadi, M. Spira, P.M. Zerwas, *Phys. Lett. B* 311 (1993) 255;
K. Melnikov, O.I. Yakovlev, *Phys. Lett. B* 312 (1993) 179;
M. Inoue, R. Najima, T. Oka, J. Saito, *Mod. Phys. Lett. A* 9 (1994) 1189;
J. Fleischer, O.V. Tarasov, *Z. Phys. C* 64 (1994) 413;
J. Fleischer, O.V. Tarasov, V.O. Tarasov, *Phys. Lett. B* 584 (2004) 294.
- [43] M. Steinhauser, in: B.A. Kniehl (Ed.), *Proceedings of the Ringberg Workshop on the Higgs Puzzle — What can we learn from LEP2, LHC, NLC, and FMC?*, Ringberg Castle, Germany, 8–13 December 1996, World Scientific, Singapore, 1997, p. 177 [arXiv:hep-ph/9612395];
K.G. Chetyrkin, B.A. Kniehl, M. Steinhauser, *Nucl. Phys. B* 510 (1998) 61 [arXiv:hep-ph/9708255].
- [44] U. Aglietti, R. Bonciani, G. Degrassi, A. Vicini, *Phys. Lett. B* 595 (2004) 432 [arXiv:hep-ph/0404071].
- [45] F. Fugel, B.A. Kniehl, M. Steinhauser, *Nucl. Phys. B* 702 (2004) 333 [arXiv:hep-ph/0405232].

- [46] G. Degrossi, F. Maltoni, Nucl. Phys. B 724 (2005) 183 [arXiv:hep-ph/0504137];
G. Passarino, C. Sturm, S. Uccirati, Phys. Lett. B 655 (2007) 298 [arXiv:0707.1401 [hep-ph]].
- [47] M. Butenschön, F. Fugel, B.A. Kniehl, Phys. Rev. Lett. 98 (2007) 071602 [arXiv:hep-ph/0612184].
- [48] M. Butenschön, F. Fugel, B.A. Kniehl, Nucl. Phys. B 772 (2007) 25 [arXiv:hep-ph/0702215].
- [49] B.A. Kniehl, A. Sirlin, Phys. Lett. B 318 (1993) 367;
B.A. Kniehl, Phys. Rev. D 50 (1994) 3314 [arXiv:hep-ph/9405299].
- [50] M.S. Chanowitz, M.A. Furman, I. Hinchliffe, Phys. Lett. 78B (1978) 285;
M.S. Chanowitz, M.A. Furman, I. Hinchliffe, Nucl. Phys. B 153 (1979) 402;
Z. Hioki, Phys. Lett. B 224 (1989) 417;
Z. Hioki, Phys. Lett. B 228 (1989) 560, Erratum;
B.A. Kniehl, Nucl. Phys. B 376 (1992) 3.
- [51] A. Djouadi, P. Gambino, Phys. Rev. Lett. 73 (1994) 2528 [arXiv:hep-ph/9406432];
K.G. Chetyrkin, B.A. Kniehl, M. Steinhauser, Phys. Rev. Lett. 78 (1997) 594 [arXiv:hep-ph/9610456];
K.G. Chetyrkin, B.A. Kniehl, M. Steinhauser, Nucl. Phys. B 490 (1997) 19 [arXiv:hep-ph/9701277].
- [52] D.A. Ross, M. Veltman, Nucl. Phys. B 95 (1975) 135;
M. Veltman, Nucl. Phys. B 123 (1977) 89;
J.J. van der Bij, F. Hoogeveen, Nucl. Phys. B 283 (1987) 477;
A. Djouadi, P. Gambino, Phys. Rev. D 49 (1994) 4705 [arXiv:hep-ph/9308338];
B.A. Kniehl, Phys. Rev. D 53 (1996) 6477 [arXiv:hep-ph/9602304].